Implication of oxidative stress in the pathogenesis of systemic sclerosis via inflammation, autoimmunity and fibrosis

Ludivine Doridot, Mohamed Jeljeli, Charlotte Chêne, Frédéric Batteux

Evaluation of performance of copper converter slag as oxygen carrier in chemical-looping combustion (CLC)

Merve Durmaz[a], Nesibe Dilmaç[a,*], Ömer Faruk Dilmaç[a]

[a]Çankırı Karatekin University, Chemical Engineering Department, 18200, Uluyazı, Çankırı, TURKEY

*Corresponding Author: ndilmac@karatekin.edu.tr

Abstract

In this study, copper converter slag sample was utilized as oxygen carrier (OC) for Chemical Looping Combustion (CLC) of synthetic syngas. The CLC cycles were substantiated in a bench-scale fluidized bed reactor by altering the inlet atmosphere between fuel and air consecutively. The tests were conducted at 4 times the minimum fluidization velocity, and 1123 K (850 ^{o}C) reduction half-cycle temperature (T_{RHC}) for 50 cycles. The mean fuel gas conversion values obtained during 30 seconds of RHC time (t_{RHC}) were as; 78% for 1:1 CO in nitrogen, 84-89% for syngas, and 97% for 1:1 H_2 in nitrogen. Copper converter slag sample was stable and sufficiently reactive throughout the tests, moreover, the reactivity increased substantially by the consecutive CLC cycles. The increase of the porosity and the formation of the copper ferrite during the CLC cycles were found to be the main contributors to the activation of the copper converter slag. It is concluded that the evaluation of copper converter slag in the CLC process is both an economical option for OC supply (especially in coal-fueled CLC processes where some OC loss is inevitable), and an environmentally favorable alternative for recycling copper converter slag unless wasting the precious metals in it.

Keywords: Chemical-looping combustion, CO_2 capture, oxygen carrier, copper converter slag, copper ferrite.

1. INTRODUCTION

Combustion of fossil fuels for electricity and heat generation is the largest single source of global CO_2 emissions [1]. Since other alternatives such as renewables and nuclear power generation seem far from substituting fossil fuels in short term, improving the utilization efficiency of fossil energy and developing CO_2 capture and storage (CCS) technologies will be the best choices for human responding to the global warming [2].

Chemical Looping Combustion (CLC), has attracted substantial attention in energy production due to its inherent CO_2 capture facility with a minimal energy penalty [3]. In this process, the combustion is split into two steps; the combustion of the fuel by lattice oxygen of the oxygen carrier (OC) in the fuel reactor (Reduction Half Cycle, RHC given in Eq.(1)) and, the regeneration of the oxygen-depleted OC by atmospheric oxygen in the air reactor (Oxidation Half Cycle, OHC given in Eq.(2)).

$$C_nH_m + Me_xO_y \rightarrow nCO_2 + \left(\frac{m}{2}\right) H_2O + Me_xO_{y-1} \quad \text{.....(1)}$$

$$Me_xO_{y-1} + \left(\frac{1}{2}\right) O_2 \rightarrow Me_xO_y \quad \text{.....(2)}$$

Mostly, the air and the fuel reactors are interconnected fluidized beds whose atmospheres are isolated by loop seals, and the OC circulates between these reactors for many full cycles whilst leading inherent CO_2 capture [4]. Essentially, the overwhelming supremacy of CLC to the other CO_2 capture technologies stems from its abovementioned ability that enables direct separation of CO_2 from the rest of the flue gases during combustion [5]. In this way, the need for additional equipment and energy demand for gas separation is eliminated, while the environmental impact is reduced. The estimated environmental performance of CLC process is given and compared with two main commercial CCS technologies in **Table-1**.

Table-1: Environmental performance of CLC process and comparison with current options [6,7]

CCS Option	Cost (US $/ton CO_2 avoided)	GWI* (kg CO_2 eq./MWh)
Post combustion CCS with amine scrubbing	36-53	180-200 (Based on fuel type)
Oxy-fuel combustion	30-67	150-200 (Based on fuel type)
CLC with a Fe-based OC	20 (Estimated value)	85 (Estimated value)

*Global Warming Impact

Although a large volume of knowledge on gas-fueled CLC has been accumulated up to date [8], recent studies on CLC technology head towards to utilization of coal due to its low cost, abundance, and high availability all over the Earth [9]. However, there are some issues about coal-fueled CLC because the process design may vary significantly according to the coal feeding type *i.e*. direct or indirect feeding. To be more clear, in case of indirect coal feeding, an external gasifier unit is essential and, in this case, the actual fuel combusted in CLC fuel reactor is the gasification product of coal instead of the coal itself (syngas CLC). The weakness of this approach is the addition of a gasifier which decreases efficiency and increases the complexity of the system [10]. On the other hand, in case of direct coal feeding, either the coal can be gasified in the fuel reactor and the gasification products can react with the solid OC (in-situ gasification CLC, iG-CLC), or a proper OC can release gaseous O_2 to react with the coal (Chemical looping with oxygen uncoupling, CLOU). Both approaches are being intensively investigated at present, but no matter which option is preferred, the OC for direct coal CLC process should be an abundant, low-cost, and reactive material since some losses are inevitable during ash separation. This situation brought some natural minerals (hematite [11], ilmenite [12–14], etc.), and industrial wastes (electric arc furnace dust [15], steel slag [16,17], electric arc furnace slag [18], red mud [8,19] and pyrite cinder [20]) into an advantageous stage as OCs in CLC. It is worth emphasizing that reutilization of the waste materials in CLC will not only reduce the supply and preparation costs of the OCs, it will also

lower the soil, water, and air contamination and reduce the charges associated with the disposal of the wastes [21].

As is known, copper slag is a by-product generated during pyrometallurgical copper extraction processes [22,23]. For every ton of metal produced, approximately 2.0-3.0 tons of slag is generated [24], and as a result of this fact, roughly 40 million tons of copper slag is discharged annually worldwide [22]. However, solely 20% [25] of that waste is reutilized as concrete aggregate, asphalt pavement, railroad ballast, ceramic tile, abrasive, mine backfill, roofing material or land reclamationer [22,24,26]. The rest is stockpiled which not only causes serious environmental pollution, but also wastes a huge amount of resources since copper slag contains a considerable amount of iron (at least 40%) [27] along with other elements like copper, zinc, and lead. From this aspect, copper slag may be regarded as a kind of costless, iron-bearing mineral source as it is discarded from copper smelting plants [28].

Taking into consideration that the iron-based materials are increasingly favored by chemical looping (CL) processes, it was thought that the utilization of copper converter slag as OC in CLC may result in a satisfying performance. Moreover, copper metal in its composition may lead to a synergistic improvement in the reactivity, while SiO_2 -the second most abundant compound - could serve as a support material improving the mechanical strength. Actually, there are a number of CL studies in the literature [29–32] in which bimetallic Cu-, and Fe-based OCs were used to take advantages of both metal oxides. Even though promising results were obtained and the OC exhibited superior reactivity over its single oxides CuO and Fe_2O_3, the common drawback for the abovementioned studies was that the "copper ferrite" ($CuFe_2O_4$) or the "copper-decorated (or doped) Fe_2O_3" OCs were prepared synthetically by using methods such as; sol-gel combustion synthesis, surface immersion or wet impregnation. To the authors' knowledge, copper converter slag is being used as OC in CLC process for the first time by means of this study without needing any preparation step. Besides, although the

interaction of the species in OCs mostly results in the formation of undesired products that lower the oxygen carrying capacity, the inherent formation of $CuFe_2O_4$ in the current study was favorable. Above all, it was thought that copper converter slag may be an economical substitute for natural iron ores which cost around 150-200 USD per ton in global markets [19].

2. EXPERIMENTAL

2.1 Copper converter slag

The copper converter slag sample used as OC in this study was supplied from Eti Bakır A.Ş. (Samsun, Türkiye). The chemical composition of the copper converter slag sample is given in **Table-2**.

Table-2: Chemical composition of the copper converter slag (%, w/w)

Fe_2O_3	SiO_2	CuO	ZnO	Al_2O_3	PbO_2	CaO	Co_3O_4	Others
49.2	28.9	8.0	4.5	2.3	1.5	0.5	0.5	4.6

The copper converter slag samples –received as lumps- were dried at 105ºC in an oven for 2 hours, then crushed in a jawbreaker and sieved. In all CLC tests, approximately 5 g of copper converter slag sample which is in the size range of 0.18-0.25 mm was used as OC.

2.2 Set-up, test procedure, and equations

The experimental set-up is shown schematically in **Figure 1** and more details can be found in our previous study [33]. To summarize briefly, the CLC tests were conducted on a bench scale, quartz fluidized bed reactor (i.d.=22 mm, length= 1200 mm) by altering the inlet atmosphere between fuel and air streams consecutively. The RHC temperature was kept at 1123 K (850 ºC) in all tests by means of a vertical tube furnace surrounding the reactor. The fuel gas compositions were as; CO and N_2 in ratio of 1:1 (V/V) (C1 in Test 1); H_2 and N_2 in ratio of 1:1 (V/V) (C2 in Test 2); CO, H_2 and N_2 in ratio of 1:1:2 (V/V)(C3 in Test 3); CO, H_2

and N_2 in ratio of 3:1:4 (V/V) (C4 in Test 4). Synthetic air (O_2 and N_2 in a ratio of 1:3.76 (V/V)) was used as the oxidizing atmosphere. The RHCs and OHCs were driven for 30 and 180 s respectively. The reactor was purged with nitrogen for 180 s after each gas switch. The volumetric flow rate of the inlet gas was 4 times the minimum fluidization velocity (u_{mf}). The details about the calculation of the u_{mf} were given in a previous study [34]. The gas traffic in each test was adjusted and controlled by the collaborative operation of the mass flow controllers (MFC, Aalborg), solenoid valves, a PLC flow controller, and software.

For a given test, copper converter slag sample was placed into the reactor and the test scenario on the software was run for 50 cycles. As the 50th OHC of the test was completed, the reactor was cooled to the room temperature under nitrogen flow.

The composition of the stack gases emitted from the reactor during the tests was determined via a gas analyzer (ABB EL 3020). The equations used for determination of the performance of the copper converter slag by means of the measured gas composition values are given below. Further explanations and details of the data evaluation can be found elsewhere [35,36]. The conversion of the OC (X) is a time-dependent variable and its instantaneous value can be calculated in terms of oxidation degree according to the Eq. (3) where m_o is the mass of the OC in its fully oxidized state, m_{red} is the mass of the OC in its fully reduced state, and m_t is the mass of the OC in any time of a given RHC/OHC.

$$X = \frac{m_t - m_{red}}{m_o - m_{red}} \quad \text{.....(3)}$$

The oxidation degree of the OC decreases during the progress of a given RHC (see **Figure 2**). Since the experimental set-up used in this study was inconvenient for determining the instantaneous mass of the OC, the conversion of the OC by the end of the ith RHC ($X_{i,red}$) was calculated depending on the fuel gas consumption (CO and H_2 mixture) as given in Eq.(4) in which "$y_{j,in}$/ $y_{j,out}$" is the instantaneous mole fraction of gas "j" at the inlet/outlet of the reactor,

$(M_A)_O$ is the atomic weight of the oxygen (16 kg.kmol^{-1}), $\dot{n}_{in}$ is the molar flow rate of the fuel (kmol.s^{-1}), and R_{OC} is the oxygen-carrying capacity of the copper converter slag. The instantaneous reduction rate of the OC (dX_i/dt) was calculated with the aid of the instantaneous stack gas composition data as given in Eq. (5) [33].

$$X_{i,red.} = X_{(i-1),oxd} - \left(\frac{(M_A)_O . \dot{n}_{in}}{m_o . R_{OC}}\right) . \int_{t_{(4i-4)}}^{t_{(4i-3)}} \left(1- \frac{y_{CO_{in}} . (y_{CO_{out}} + y_{H_{2out}})}{(y_{CO_{out}} + y_{CO_{2out}})}\right) .dt \quad \text{.....(4)}$$

$$\frac{dX_{i,red.}}{dt} = -\left(\frac{(M_A)_O . \dot{n}_{in}}{m_o . R_{OC}}\right) . \left(1- \frac{y_{CO_{in}} . (y_{CO_{out}} + y_{H_{2out}})}{(y_{CO_{out}} + y_{CO_{2out}})}\right) \quad \text{.....(5)}$$

The instantaneous and mean conversion efficiency values of CO and H_2 (γ) were calculated according to the Eq.(6), Eq.(7), Eq.(8), and Eq.(9) respectively [33].

$$\gamma_{CO}(t) = \left[\frac{y_{CO_{2out}}}{y_{CO_{out}} + y_{CO_{2out}}}\right] \quad \text{.....(6)}$$

$$\gamma_{H_2}(t) = \left[1- \frac{\dot{n}_{out} . y_{H_{2out}}}{\dot{n}_{in} . y_{H_{2in}}}\right] \quad \text{.....(7)}$$

$$(\overline{\gamma_{CO}})_{i^{th}\ RHC} = \left[\frac{\sum_{n=1}^{30} [\gamma_{CO}(t)]_n}{30}\right] (t_{RHC}=30\ s) \quad \text{.....(8)}$$

$$\left(\overline{\gamma_{H_2}}\right)_{i^{th}\ RHC} = \left[\frac{\sum_{n=1}^{30}\left[\gamma_{H_2}(t)\right]_n}{30}\right](t_{RHC}=30\ s)\ldots\ldots(9)$$

The solid recirculation rate ($\dot{m}_{ox}$) value for the copper converter slag, *i.e* the mass of the fully oxidized OC that is required to be circulated between fuel and air reactors of a 1 $MW_{th\ (STD\ conditions)}$ syngas fuelled CLC unit per second, was calculated according to the Eq.(10). The "φ_{power}" seen on Eq.(10) was calculated according to the Eq.(11) in which $\Delta H^{o}_{combustion}$ is the standard combustion heat of fuel gas (kJ/s) [33].

$$\dot{m}_{ox}= \frac{(M_A)_O \cdot \dot{n}_{fuel,in} \cdot \left(\overline{\gamma_{fuel}}\right)_{All\ RHCs} \cdot \varphi_{power}}{R_{OC} \cdot \Delta X_{OC}}\ldots\ldots(10)$$

$$\varphi_{power}= \frac{1000\ (kJ/s)}{\Delta H^{o}_{combustion} \cdot \dot{n}_{fuel,in}}\ldots\ldots(11)$$

The solid inventory (m_{solid}) value for the copper converter slag, *i.e* the mass of the fully oxidized OC that is required to be located into a 1 $MW_{th\ (STD\ conditions)}$ syngas fuelled CLC unit, was calculated according to the Eq. (12) [33].

$$m_{solid}= \frac{\varphi_{power} \cdot m_O}{\left(\overline{\gamma_{fuel}}\right)_{All\ RHCs}}\ldots\ldots(12)$$

3. RESULTS AND DISCUSSIONS

The "t vs % (v/v)" graphs showing the variation of the stack gas compositions during **Test 1**, **Test 2**, **Test 3**, and **Test 4** are given in **Figure 3** and **Figure 4** respectively. The mean reduction degree ($(\overline{R\%})_{\text{All RHCs}}$), mean fuel conversion efficiency ($(\overline{\gamma_{\text{fuel}}})_{\text{All RHCs}}$), solid recirculation rate ($\dot{m}_{ox}$), and solid inventory (m_{solid}) values of copper converter slag for each test were determined by the help of the equations given in the previous section and the results are given at **Table-3**.

Table-3. The mean reduction degree, mean fuel conversion efficiency, solid recirculation rate and solid inventory values for copper converter slag (R%=100×(1-X))

Test	Fuel composition	Volumetric and molar rates of fuel	W_{th} of reactor	$(\overline{R})_{\text{All RHCs}}$ (%)	$(\overline{\gamma_{\text{fuel}}})_{\text{All RHCs}}$ (×100)	$\dot{m}_{ox}$ (kg/s)	m_{solid} (kg/MW_{th})
1	$CO+N_2$ with 1:1 molar ratio (C1)	518 (ml/min.) 0.000352 (mole/s)	49.81	8.84	77.59	3.04	129.38
2	H_2+N_2 with 1:1 molar ratio (C2)	682 (ml/min.) 0.000465 (mole/s)	66.50	13.27	97.31	2.52	77.27
3	$CO+H_2+N_2$ with 1:1:2 molar ratio (C3)	588 (ml/min.) 0.000400 (mole/s)	56.9	10.52	88.97	2.91	98.76
4	$CO+H_2+N_2$ with 3:1:4 molar ratio (C4)	552 (ml/min.) 0.000376 (mole/s)	53.35	9.36	84.13	3.11	111.41

Main findings can be listed as below;

3.1 Carbon deposition

No carbon deposition was observed during the RHCs of the tests. Otherwise, as soon as the carbon contaminated copper converter slag got in touch with the oxygen, an increment on CO_2 concentration would have appeared on OHC regions of the "t vs % (v/v)" graphs.

3.2 Increase on reactivity

The copper converter slag kept its reactivity more than 8 hours (50 cycles) and exhibited remarkable "activation behavior" characterized by lowering CO and H_2 peaks and increasing CO_2 peaks during progressing RHCs as seen in **Figure 3** and **Figure 4**. The "activation" was

more appreciable during hydrogen conversion. This may be attributed to the micro-scale alterations occurred on slag structure owing to the repeating CLC cycles. To be more clear, because of the "hematite to magnetite" transformations during RHCs, the oxygen lattice changed from close-packed hexagonal to face-centered cubic. As a result, the particle swelled, the reacting surface area increased, and the access of the CO and/or H_2 to the active sites was eased [34].

A more detailed graph (**Figure 5**) representing the variation of the fuel gas conversion throughout the tests reveals the abovementioned "activation behavior" more clearly. As seen in **Figure 5**, fuel gas conversion efficiency improved dramatically by the first one or two full cycles of the tests. The improvement was more sensible for **Test 2** and **Test 3** whose hydrogen concentrations were higher. This may be related to the small size of the hydrogen molecules.

The change of the reduction rate of copper converter slag versus the oxidation degree through the 1^{st}, 5^{th}, 10^{th}, 25^{th} and 50^{th} RHCs of all tests can be seen on **Figure 6**. The reduction rate was in its highest value at the first seconds of a given RHC but as the reduction time elapsed, the reduction rate decreased. As a common fact for all tests, while the decrease seen on reduction rate was severe for the 1^{st} RHC, it was slighter for subsequent RHCs. In other words, as a given test moved forward from 1^{st} RHC towards 50^{th} RHC, the reduction rate of copper converter slag became more stable and resistant to decrease. It is worth emphasizing that, the abovementioned progress seen on reduction rate was more distinct in presence of H_2 such that the 50^{th} RHCs of **Test 2** and **Test 3** proceeded with almost the same reduction rate from the beginning of the RHC to the end.

The activation of copper converter slag during oxidation was slighter compared to the reduction and it was almost restricted by the first OHCs for all tests (see **Figure 3** and **Figure 4**).

3.3 Structural changes

Figure 7 represents the structures of the copper converter slag particles before and after being used for 50 full cycles in **Test 1, Test 2, Test 3** and **Test 4** respectively. In original form, copper converter slag particles were dense, compact and nearly plain surfaced as seen in **Figure 7**. In fact, the low fuel and air conversion values obtained during the first reduction and oxidation half cycles of the tests (see **Figure 3** and **Figure 4**) may be attributed to this fact. On the other hand, SEM images of the processed particles significantly differ from the images of the unprocessed ones. The dense and compact structure transformed into a highly porous texture and the sharp edges were smoothed. The enormous increase occurred on porosity must have increased both the number of active sites and as well the access of the reactant gases to the active sites.

Figure 8 represents the XRD diffractograms of the copper converter slag particles before and after being used for 50 full cycles in **Test 1, Test 2, Test 3** and **Test 4** respectively. The main crystal phases of unprocessed copper converter slag are fayalite and magnetite [22,24,25,28,37–39] as seen in **Figure 8.** On the other hand, the XRD diffractograms of the processed samples indicate the existence of copper ferrite ($CuFe_2O_4$) [29,30,40–45] which has received great attention recently due to its interesting electrical, magnetic, optic and catalytic properties [42,44,46,47]. In this sense, the "activation" of copper converter slag may be partially attributed to the formation of copper ferrite since a number of earlier studies [29,30] verify that $CuFe_2O_4$ OC not only overcomes the disadvantages of a single CuO or Fe_2O_3 OC, but also shows beneficial synergistic effects on the reactivity of the OC [29].

The FTIR spectra of all samples were recorded to further testify the formation of $CuFe_2O_4$ (**Figure 9**). The peaks at 560 and 470 cm^{-1} in **Figure 9-a** stem from Fe-O stretching in magnetite (Fe_3O_4) and asymmetric Si-O bending in amorphous SiO_2, respectively. The peak seen at 1100 cm^{-1} in each curve indicates the presence of amorphous SiO_2, and it is due to Si-

O stretching. On the other hand, the peak seen at 870 cm^{-1} in **Figure 9-a** is due to the asymmetric stretching of Si-O bond in fayalite ($FeSiO_4$). Since the fayalite in copper converter slag was decomposed as a result of CLC cycles –as proven by XRD results-, the peak seen at 870 cm^{-1} in **Figure 9-a** disappeared on the other curves. Instead, the peak seen at 1100 cm^{-1} in **Figures 9-b, c, d,** and **e** was intensified due to the amorphous SiO_2 released by the decomposition of fayalite. Lastly, two characteristic peaks appearing at 570 and 460 cm^{-1} in **Figure 9-b, c, d,** and **e** confirm the presence of $CuFe_2O_4$ since the first peak stems from the stretching vibration of Fe^{+3}-O bond at the tetrahedral site and the latter is due to the stretching vibration of the octahedral metal (Cu^{+2}) complex, respectively [41,44,45,47–49]. Examining the XRD and FTIR results together, it can be concluded that, fayalite in copper converter slag was decomposed and copper ferrite was generated owing to the CLC process.

5. CONCLUSIONS

In this study, copper converter slag was used as OC in gas-fueled CLC process. The reactivity of copper converter slag increased remarkably during the progressing RHCs and the increase was more distinct in the case of H_2 in fuel gas. To clarify the reason for that situation, structural analyses were performed. It was clearly seen from the SEM images that the porosity of copper converter slag grains increased significantly after the CLC tests. This fact is more likely to have an impact on the abovementioned "activation behavior". On the other hand, the XRD and FTIR analyses revealed the presence of copper ferrite ($CuFe_2O_4$) in the processed samples. Since $CuFe_2O_4$ was proven to be an OC with promising performance, the "activation" of copper converter slag in the current work was partially attributed to the formation of $CuFe_2O_4$. From all aspects explained thus far, it is possible to say that copper converter slag is a promising OC candidate which exhibits a "self-enhancing" CLC performance. Besides, utilization of copper converter slag as OC in CLC may also counteract

the financial and environmental concerns since it may contribute to the reutilization of an industrial waste.

Acknowledgements

This study was funded by TUBITAK under research project grant 113M548, and performed in Çankırı Karatekin University. These supports are thankfully acknowledged. The authors are also grateful to Ali YILMAZ and Mehmet CAMBAZOĞLU from Eti Bakır A.Ş (Samsun-Türkiye) for supplying the copper converter slag samples, and Dr. Baran ÖNAL ULUSOY for valuable discussions.

REFERENCES

[1] United States Environmental Protection Agency (EPA), Global Gas Emissions Data. https://www.epa.gov/ghgemissions/global-greenhouse-gas-emissions-data (Accessed July 18, 2019).

[2] Deng G, Li K, Gu Z, Zhu X, Wei Y, Cheng X, et al. Synergy effects of combined red muds as oxygen carriers for chemical looping combustion of methane. Chem Eng J 2018. doi:10.1016/j.cej.2018.02.072.

[3] Matzen M, Pinkerton J, Wang X, Demirel Y. Use of natural ores as oxygen carriers in chemical looping combustion: A review. Int J Greenh Gas Control 2017;65:1–14. doi:10.1016/j.ijggc.2017.08.008.

[4] Abad A, Mendiara T, Gayán P, García-Labiano F, De Diego LF, Bueno JA, et al. Comparative Evaluation of the Performance of Coal Combustion in 0.5 and 50 kWth Chemical Looping Combustion Units with Ilmenite, Redmud or Iron Ore as Oxygen Carrier. Energy Procedia 2017;114:285–301. doi:10.1016/j.egypro.2017.03.1170.

[5] Chen L, Bao J, Kong L, Combs M, Nikolic HS, Fan Z, et al. The direct solid-solid reaction between coal char and iron-based oxygen carrier and its contribution to solid-fueled chemical looping combustion. Appl Energy 2016;184:9–18. doi:10.1016/j.apenergy.2016.09.085.

[6] Cuéllar-Franca RM, Azapagic A. Carbon capture, storage and utilisation technologies: A critical analysis and comparison of their life cycle environmental impacts. J CO2 Util 2015;9:82–102. doi:10.1016/j.jcou.2014.12.001.

[7] Fan J, Hong H, Jin H. Power Generation Based on Chemical Looping Combustion: Will It Qualify to Reduce Greenhouse Gas Emissions from Life-Cycle Assessment? ACS Sustain Chem Eng 2018;6:6730–7. doi:10.1021/acssuschemeng.8b00519.

[8] Mendiara T, Abad A, De Diego LF, García-Labiano F, Gayán P, Adánez J. Use of an Fe-based residue from alumina production as an oxygen carrier in chemical-looping combustion. Energy and Fuels 2012;26:1420–31. doi:10.1021/ef201458v.

[9] Ströhle J, Orth M, Epple B. Chemical looping combustion of hard coal in a 1 MWthpilot plant using ilmenite as oxygen carrier. Appl Energy 2015;157:288–94. doi:10.1016/j.apenergy.2015.06.035.

[10] Xiao R, Song Q, Song M, Lu Z, Zhang S, Shen L. Pressurized chemical-looping combustion of coal with an iron ore-based oxygen carrier. Combust Flame 2010;157:1140–53. doi:10.1016/j.combustflame.2010.01.007.

[11] Song T, Shen T, Shen L, Xiao J, Gu H, Zhang S. Evaluation of hematite oxygen carrier in chemical-looping combustion of coal. Fuel 2013;104:244–52. doi:10.1016/j.fuel.2012.09.030.

[12] Adánez J, Cuadrat A, Abad A, Gayán P, Diego LFD, García-Labiano F. Ilmenite activation during consecutive redox cycles in chemical-looping combustion. Energy and Fuels 2010;24:1402–13. doi:10.1021/ef900856d.

[13] Berguerand N, Lyngfelt A. Chemical-looping combustion of petroleum coke using ilmenite in a 10 kwth unit-high-temperature operation. Energy and Fuels

2009;23:5257–68. doi:10.1021/ef900464j.

[14] Cuadrat A, Abad A, Adánez J, De Diego LF, García-Labiano F, Gayán P. Behavior of ilmenite as oxygen carrier in chemical-looping combustion. Fuel Process Technol 2012;94:101–12. doi:10.1016/j.fuproc.2011.10.020.

[15] Kuo YL, Huang WC, Tseng YH, Chang SH, Ku Y, Lee HY. Electric arc furnace dust as an alternative low-cost oxygen carrier for chemical looping combustion. J Hazard Mater 2018;342:297–305. doi:10.1016/j.jhazmat.2017.08.024.

[16] Di Z, Cao Y, Yang F, Cheng F, Zhang K. Studies on steel slag as an oxygen carrier for chemical looping combustion. Fuel 2018;226:618–26. doi:10.1016/j.fuel.2018.04.047.

[17] Hildor F, Mattisson T, Leion H, Linderholm C, Rydén M. Steel converter slag as an oxygen carrier in a 12 MWth CFB boiler – Ash interaction and material evolution. Int J Greenh Gas Control 2019;88:321–31. doi:10.1016/j.ijggc.2019.06.019.

[18] Dilmaç ÖF, Dilmaç N, Doruk TE. Performance of EAF slag as oxygen carrier in Chemical Looping Combustion. 14th Int. Combust. Symp. (INCOS-14 , April 25-27), Karabük-Türkiye: 2018.

[19] Mendiara T, Gayán P, Abad A, de Diego LF, García-Labiano F, Adánez J. Performance of a bauxite waste as oxygen-carrier for chemical-looping combustion using coal as fuel. Fuel Process Technol 2013;109:57–69. doi:10.1016/j.fuproc.2012.09.038.

[20] Zhang S, Rajendran S, Henderson S, Zeng D, Xiao R, Bhattacharya S. Use of pyrite cinder as an iron-based oxygen carrier in coal-fueled chemical looping combustion. Energy and Fuels 2015;29:2645–55. doi:10.1021/acs.energyfuels.5b00194.

[21] Tsakiridis PE, Agatzini-Leonardou S, Oustadakis P. Red mud addition in the raw meal for the production of Portland cement clinker. J Hazard Mater 2004;116:103–10. doi:10.1016/j.jhazmat.2004.08.002.

[22] Feng Y, Kero J, Yang Q, Chen Q, Engström F, Samuelsson C, et al. Mechanical activation of granulated copper slag and its influence on hydration heat and compressive strength of blended cement. Materials (Basel) 2019;12. doi:10.3390/ma12050772.

[23] Parada F, Parra R, Marquez F, Jara R, Carrasco JC, Palacios J. Management of copper pyrometallurgical slags : giving additional value to copper mining industry. Management 2004:543–50.

[24] Fan Y, Shibata E, Iizuka A, Nakamura T. Crystallization behaviors of copper smelter slag studied using time-temperature-transformation diagram. Mater Trans 2014;55:958–63. doi:10.2320/matertrans.M-M2014819.

[25] Guo Z, Zhu D, Pan J, Wu T, Zhang F. Improving beneficiation of copper and iron from copper slag by modifying the molten copper slag. Metals (Basel) 2016;6. doi:10.3390/met6040086.

[26] Lykasov AA, Ryss GM, Sharafutdinov DG, Pogodin AY. Extraction of iron from copper-plant slag. Steel Transl 2016;46:609–13. doi:10.3103/S0967091216090059.

[27] Khalid MK, Hamuyuni J, Agarwal V, Pihlasalo J, Haapalainen M, Lundström M. Sulfuric acid leaching for capturing value from copper rich converter slag. J Clean Prod 2019;215:1005–13. doi:10.1016/j.jclepro.2019.01.083.

[28] Cao Z, Sun T, Xue X, Liu Z. Iron recovery from discarded copper slag in a RHF direct reduction and subsequent grinding/magnetic separation process. Minerals 2016;6. doi:10.3390/min6040119.

[29] Wang B, Zhao H, Zheng Y, Liu Z, Zheng C. Chemical Looping Combustion of Petroleum Coke with CuFe2O4 as Oxygen Carrier. Chem Eng Technol 2013;36:1488–95. doi:10.1002/ceat.201200638.

[30] Wang B, Ma Q, Wang W, Zhang C, Mei D, Zhao H, et al. Effect of Reaction Temperature on the Chemical Looping Combustion of Coal with CuFe2O4 Combined Oxygen Carrier. Energy and Fuels 2017;31:5233–45. doi:10.1021/acs.energyfuels.6b02525.

[31] Yang W, Zhao H, Ma J, Mei D, Zheng C. Evaluation of copper-decorated hematite as oxygen carrier in chemical looping combustion of coal. Int Conf Power Eng 2013, ICOPE 2013 2013.

[32] Liu C, Wang W. Chemical looping gasification of pyrolyzed biomass and coal char with copper ferrite as an oxygen carrier. J Renew Sustain Energy 2018;10. doi:10.1063/1.5040379.

[33] Dilmaç N, Dilmaç ÖF, Yardımcı E. Utilization of Menteş iron ore as oxygen carrier in Chemical-Looping Combustion. Energy 2017;138. doi:10.1016/j.energy.2017.07.126.

[34] Dİlmaç N, Yörük S, Gülaboğlu ŞM. Investigation of Direct Reduction Mechanism of Attepe Iron Ore by Hydrogen in a Fluidized Bed. Metall Mater Trans B Process Metall Mater Process Sci 2015;46. doi:10.1007/s11663-015-0409-8.

[35] Dilmaç N, Dilmaç Ö. Utilization of Kayseri- Menteş iron ore as oxygen carrier in chemical looping combustion of syngas: Deconvolution of the gas analysis data. 8th Int. Exergy, Energy Environ. Symp. (IEEES-8, May 1-4), Antalya-Türkiye: 2016.

[36] Abad A, García-Labiano F, de Diego LF, Gayán P, Adánez J. Reduction kinetics of Cu-, Ni-, and Fe-based oxygen carriers using syngas (CO + H2) for chemical-looping combustion. Energy and Fuels 2007;21:1843–53. doi:10.1021/ef070025k.

[37] Chen JH, Mi WJ, Chen HY, Li B, Chou KC, Hou XM. Iron oxide recovery from fayalite in water vapor at high temperature. J Min Metall Sect B Metall 2018;54:1–8. doi:10.2298/JMMB160926011C.

[38] Zhou H, Li B, Wei Y, Wang H, Yang Y, McLean A. Magnetite reduction in copper converter slag using biodiesel produced from waste cooking oil. Can Metall Q 2019;58:187–95. doi:10.1080/00084433.2018.1540088.

[39] Michailova I, Mihailova I, Mehandjiev D. Characterization of Fayalite from Copper Slags. J Univ Chem Technol Metall 2010;45:317–26.

[40] Maleki Z, Rasouli N, Movahedi M, Sadeghi Z. Available online www.jsaer.com Research Article An efficient and magnetically separable heteropoly acid catalyst for the synthesis of β - amino carbonyl compounds under solvent-free conditions

2016;3:192–202.

[41] Kumar A, Rout L, Achary LSK, Dhaka RS, Dash P. Greener Route for Synthesis of aryl and alkyl-14H-dibenzo [a.j] xanthenes using Graphene Oxide-Copper Ferrite Nanocomposite as a Recyclable Heterogeneous Catalyst. Sci Rep 2017;7. doi:10.1038/srep42975.

[42] Rashad MM, Mohamed RM, Ibrahim MA, Ismail LFM, Abdel-Aal EA. Magnetic and catalytic properties of cubic copper ferrite nanopowders synthesized from secondary resources. Adv Powder Technol 2012;23:315–23. doi:10.1016/j.apt.2011.04.005.

[43] Kang KS, Kim CH, Cho WC, Bae KK, Woo SW, Park CS. Reduction characteristics of CuFe2O4 and Fe3O4 by methane; CuFe2O4 as an oxidant for two-step thermochemical methane reforming. Int J Hydrogen Energy 2008;33:4560–8. doi:10.1016/j.ijhydene.2008.05.054.

[44] Vergis BR, Hari Krishna R, Kottam N, Nagabhushana BM, Sharath R, Darukaprasad B. Removal of malachite green from aqueous solution by magnetic CuFe2O4 nano-adsorbent synthesized by one pot solution combustion method. J Nanostructure Chem 2018;8:1–12. doi:10.1007/s40097-017-0249-y.

[45] Kanagaraj M, Sathishkumar P, Selvan GK, Kokila IP, Arumugam S. Structural and magnetic properties of cufe2o4 as-prepared and thermally treated spinel nanoferrites. Indian J Pure Appl Phys 2014;52:124–30.

[46] Dhanda R, Kidwai M. Magnetically separable CuFe2O4/reduced graphene oxide nanocomposites: As a highly active catalyst for solvent free oxidative coupling of amines to imines. RSC Adv 2016;6:53430–7. doi:10.1039/c6ra08868f.

[47] Selvan RK, Augustin CO, Berchmans LC, Saraswathi R. Combustion synthesis of $CuFe_2O_4$. Mater Res Bull 2003; 38: 41-54.

[48] Zhang H, Gao S, Shang N, Wang C, Wang Z. Copper ferrite-graphene hybrid: A highly efficient magnetic catalyst for chemoselective reduction of nitroarenes. RSC Adv 2014;4:31328–32. doi:10.1039/c4ra05059b.

[49] Nikolov A, Titorenkova R, Velinov N, Delcheva Z. Characterization of a novel geopolymer based on acid-activated fayalite slag from local copper industry. Bulg Chem Commun 2018;50:54–61.

FIGURES

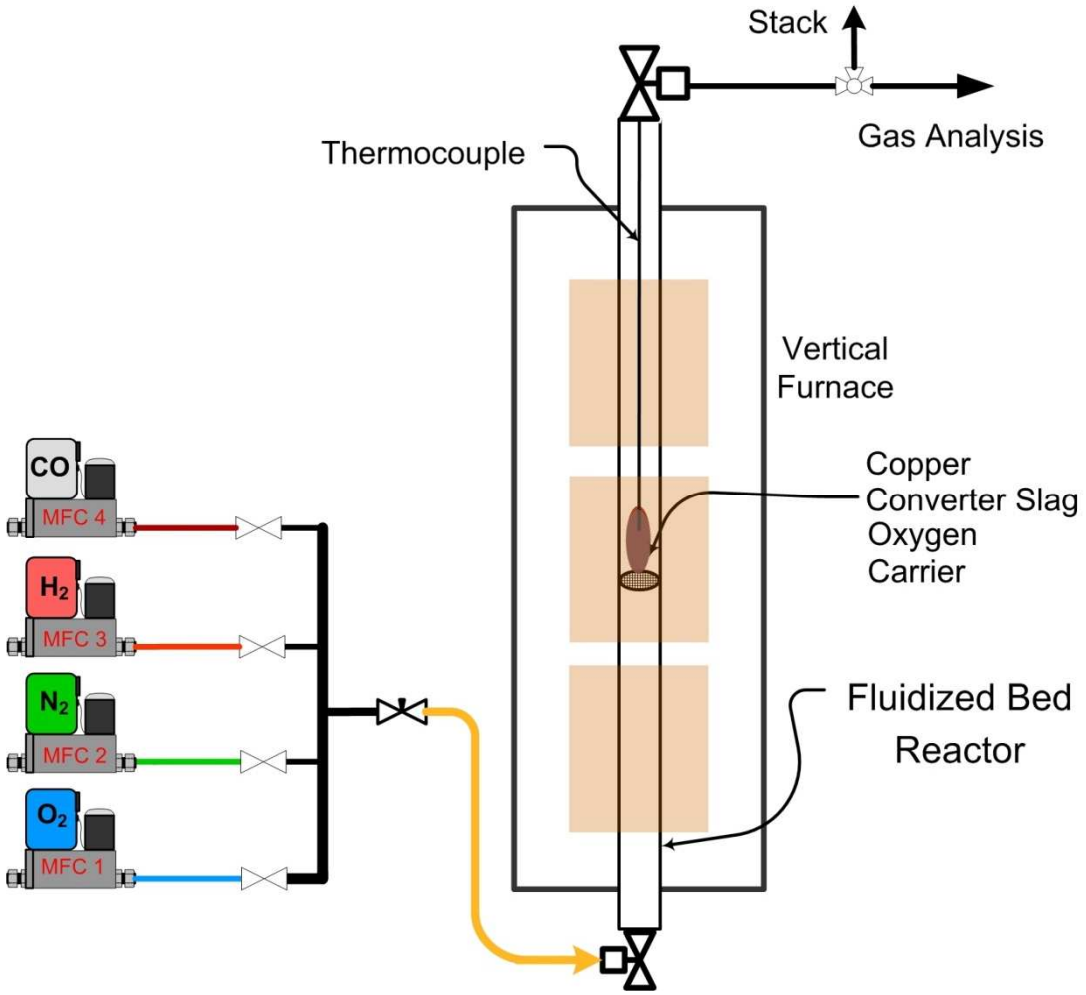

Figure 1. The scheme of CLC experimental set-up

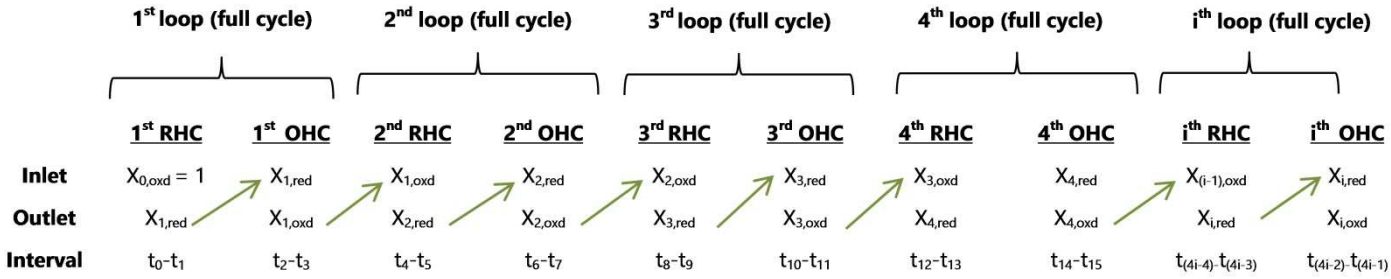

Figure 2. Variation of "X" throughout the CLC cycles

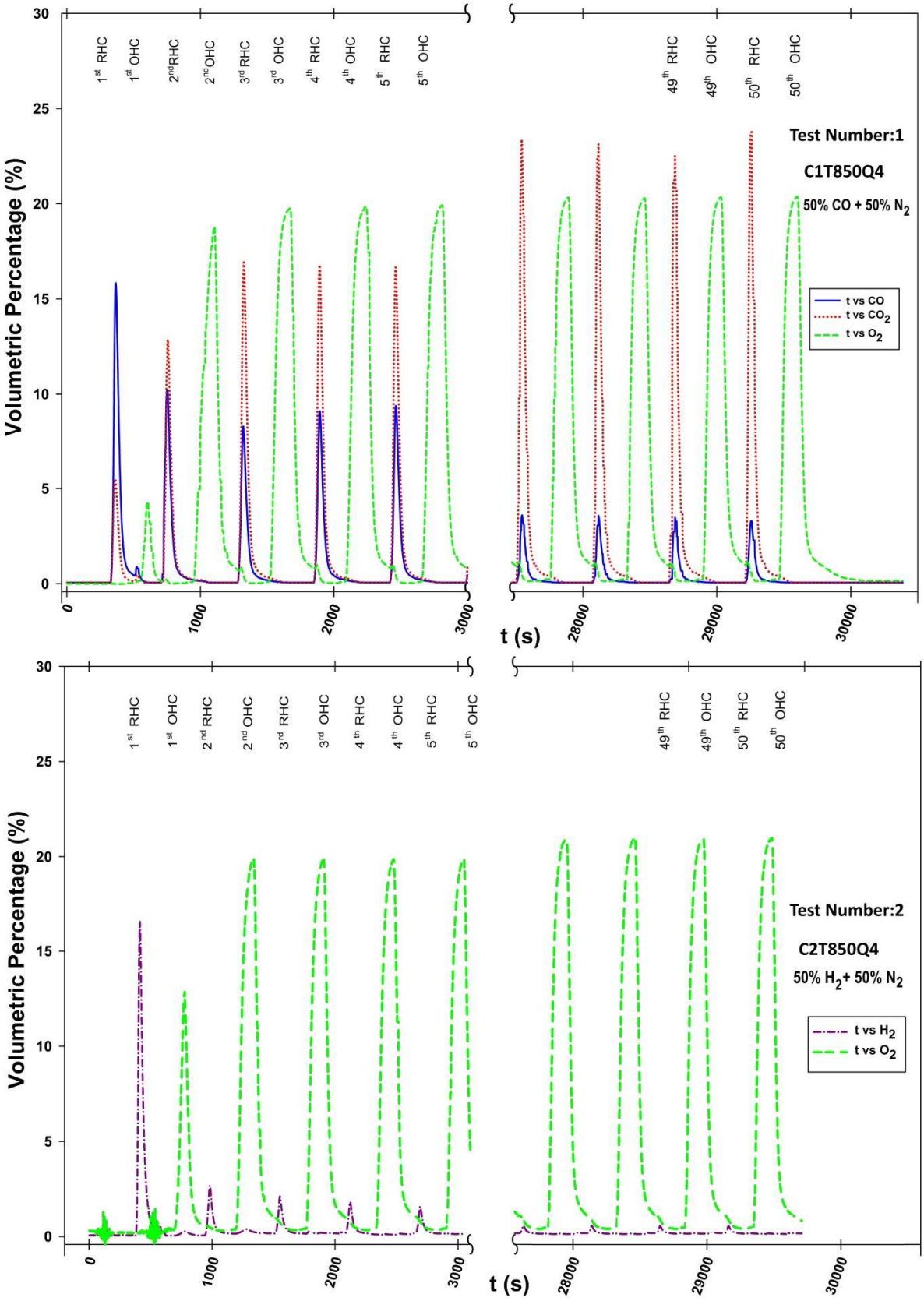

Figure 3. "t vs % (v/v)" graphs showing the variation of stack gas compositions during **Test 1** and **Test 2**

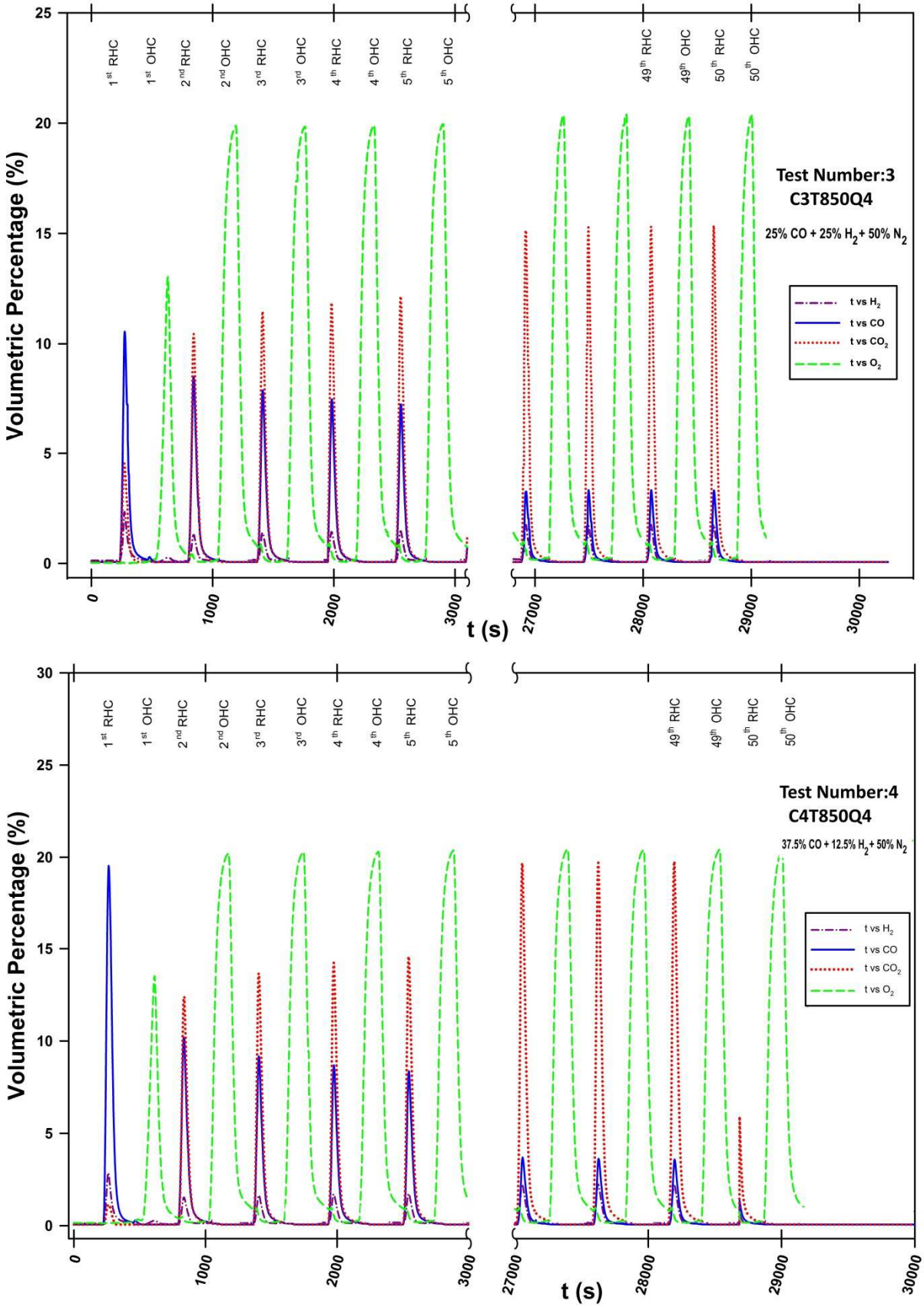

Figure 4. "t vs % (v/v)" graphs showing the variation of stack gas compositions during **Test 3** and **Test 4**

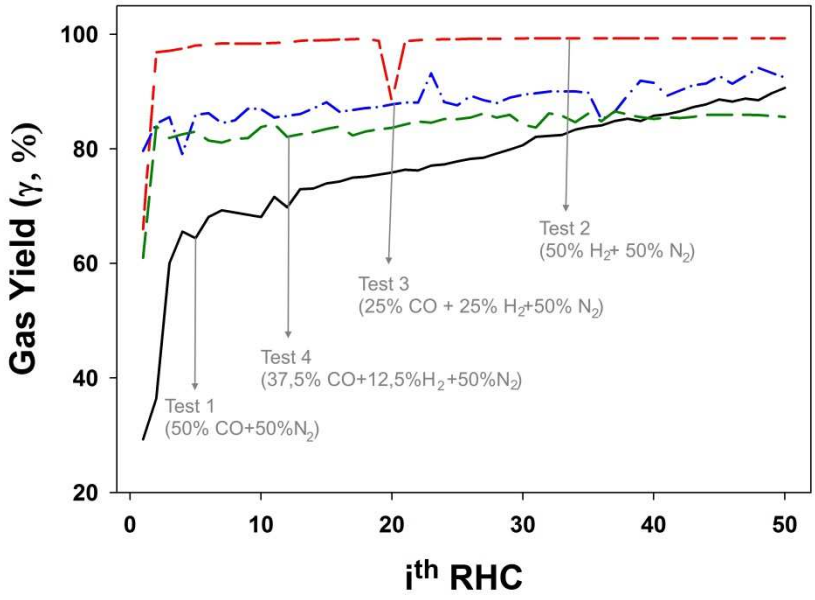

Figure 5. Variation of the gas yield throughout the tests performed in this study

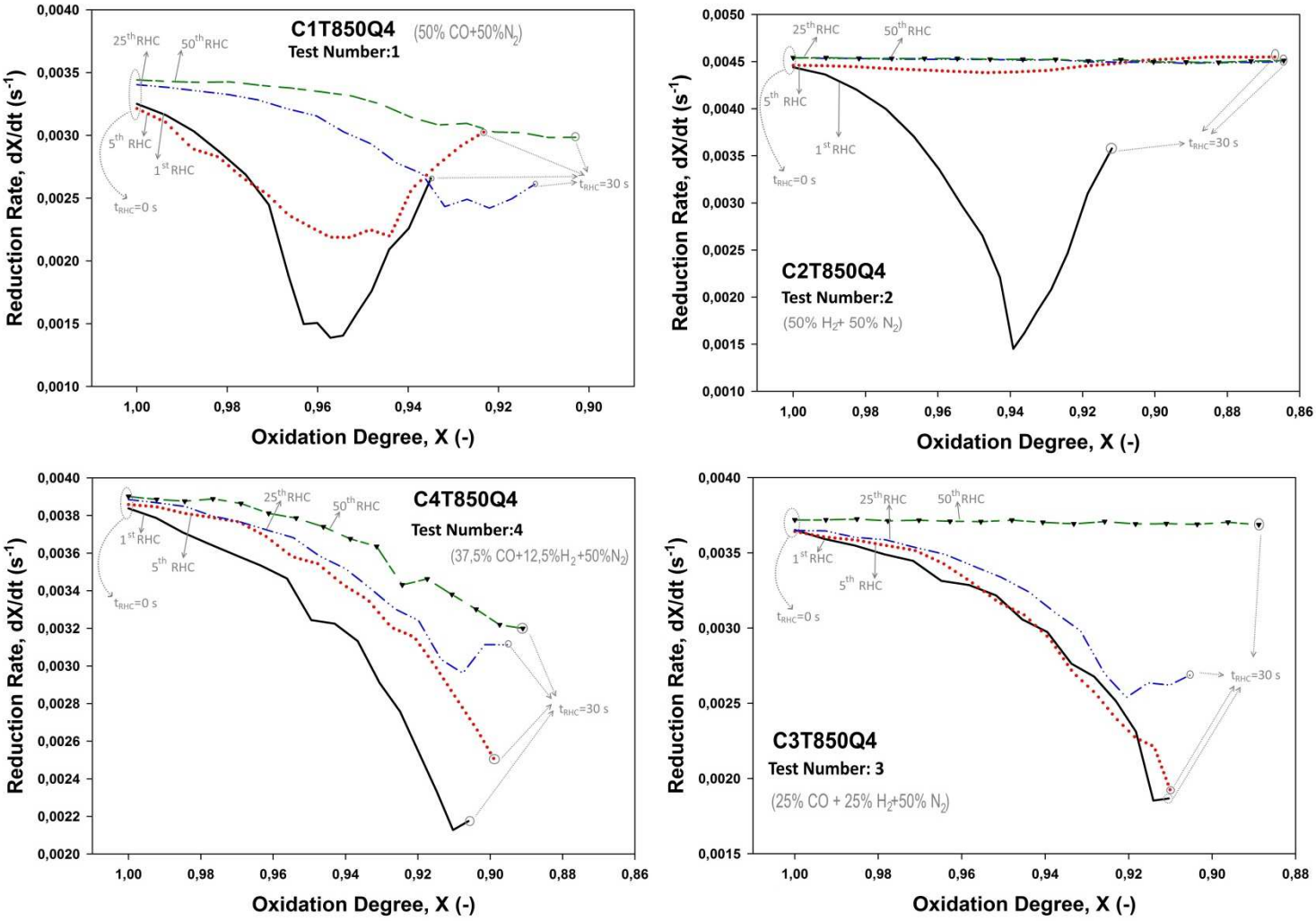

Figure 6. "X vs Reduction Rate" graphs for the tests performed in this study

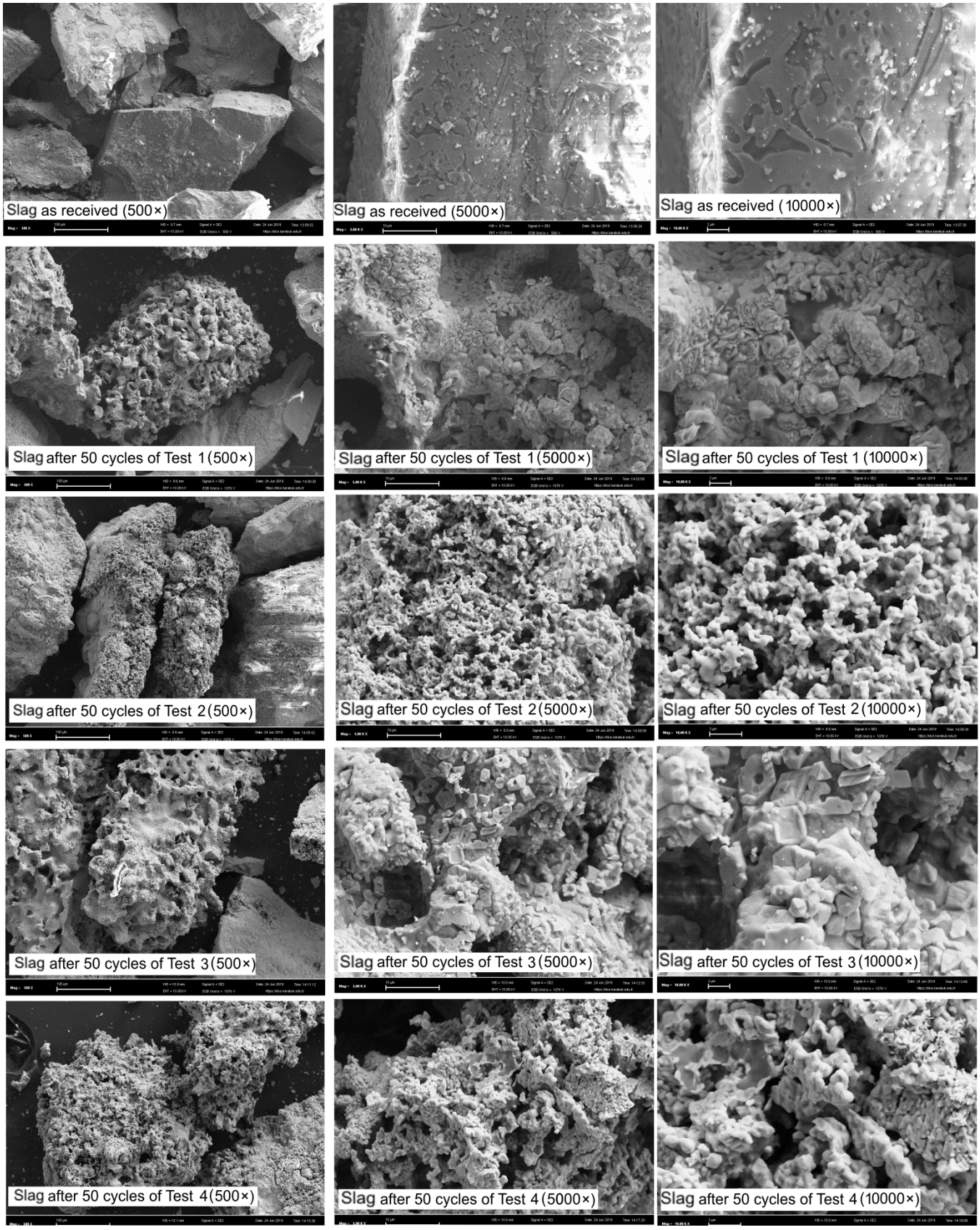

Figure 7. SEM images of copper converter slag before and after being used in CLC tests in this study

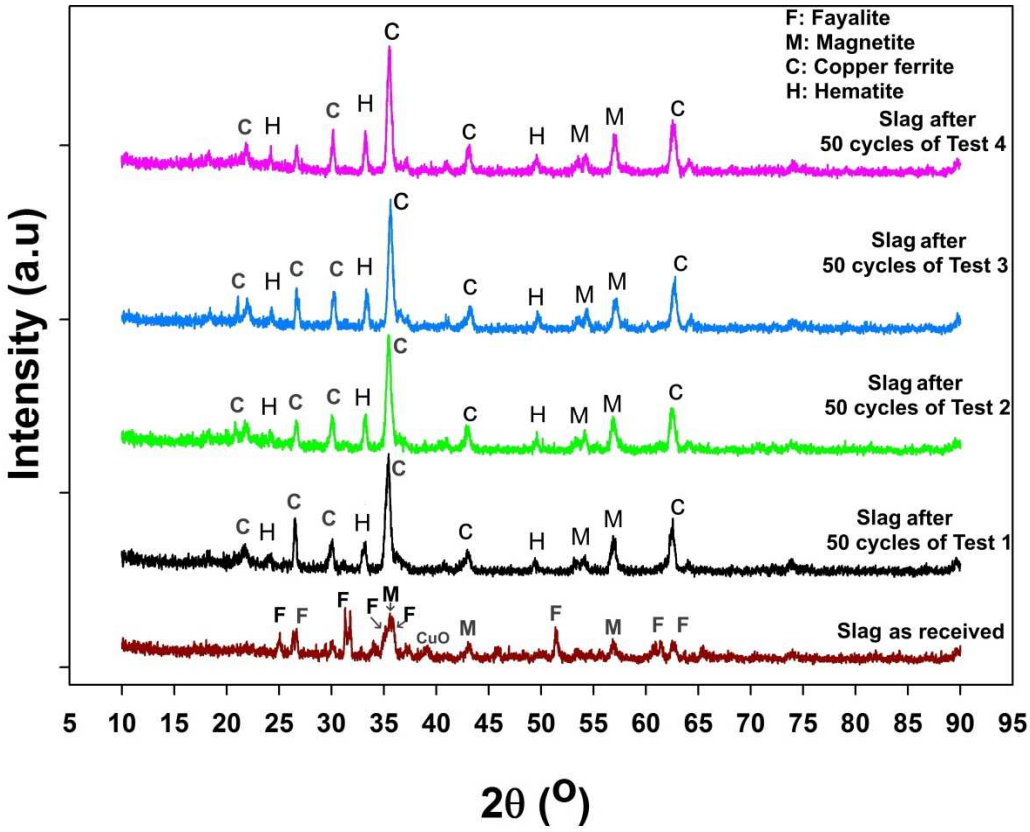

Figure 8. XRD diffractograms of copper converter slag before and after being used in CLC tests in this study

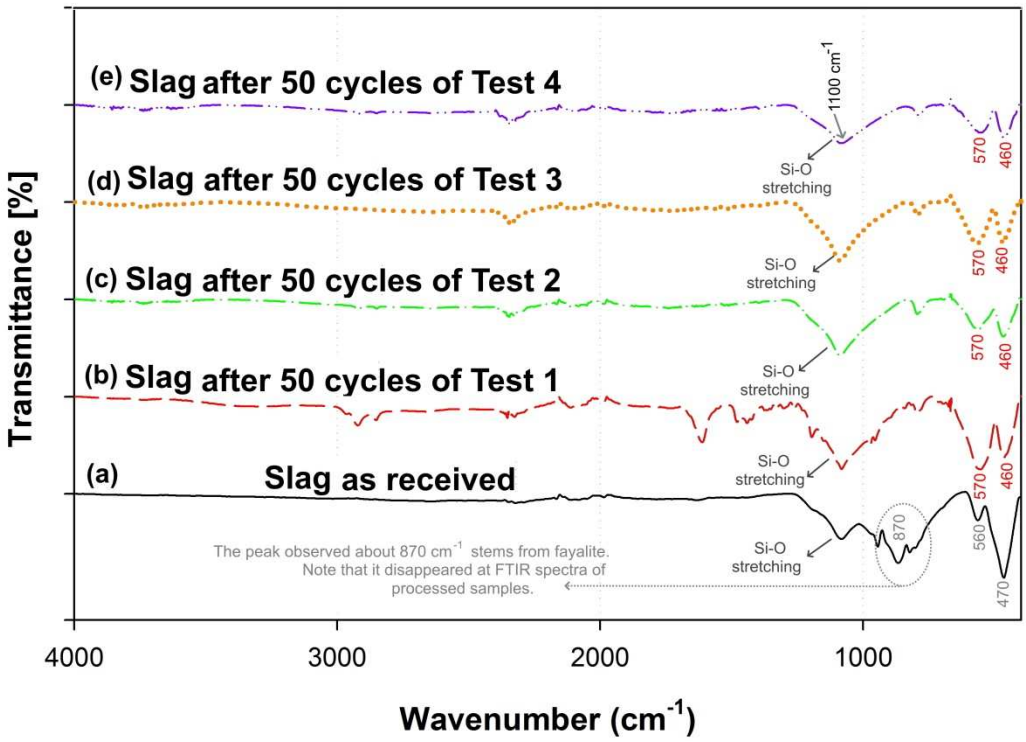

Figure 9. FTIR spectra of copper converter slag before and after being used in CLC tests in this study